Molecular Crystals and Liquid Crystals Incorporating Nonlinear Optics

Publication details, including instructions for authors and subscription information:
http://www.tandfonline.com/loi/gmcl17

Zero and Applied Field Mossbauer Spectroscopy Studies of Strong and Weak Ferromagnetic Interactions in Inorganic and Organometallic Solids

William M. Reiff [a]

[a] Department of Chemistry, Northeastern University, Boston, Massachusetts, 02115

Version of record first published: 22 Sep 2006.

To cite this article: William M. Reiff (1989): Zero and Applied Field Mossbauer Spectroscopy Studies of Strong and Weak Ferromagnetic Interactions in Inorganic and Organometallic Solids, Molecular Crystals and Liquid Crystals Incorporating Nonlinear Optics, 176:1, 391-413

To link to this article: http://dx.doi.org/10.1080/00268948908037497

Mol. Cryst. Liq. Cryst., Vol. 176, pp. 391–414
Reprints available directly from the publisher
Photocopying permitted by license only

Printed in the United States of America

ZERO AND APPLIED FIELD MOSSBAUER SPECTROSCOPY STUDIES OF STRONG AND WEAK FERROMAGNETIC INTERACTIONS IN INORGANIC AND ORGANOMETALLIC SOLIDS.

William M. Reiff
Department of Chemistry, Northeastern University,
Boston, Massachusetts 02115.

Abstract The use of zero and applied field Mossbauer spectroscopy in the study of ferromagnetic interactions in the solid state is reviewed. The angular intensity factors relevant to magnetic hyperfine splitting and cooperative magnetic ordering for the I = 1/2 —> I = 3/2 transition of Iron-57 are presented. The following examples are then considered: (a) very strong ferromagnetic interactions in metallic α-iron, (T critical) ~ 1043K, (b) very weak ferromagnetic interactions, T (critical) ~ 1K, for ionic fluorides of high spin iron III, (c) studies of highly anisotropic 1D chain metamagnets with direct spectroscopic observation of magnetization of ferromagnetic chains in small external fields, and finally (d) slow paramagnetic relaxation and ferromagnetism in dimers based on the low-spin iron III (spin doublet) centers of decamethylferrocenium units.

INTRODUCTION

The study of magnetic interactions in solids has traditionally focused primarily on bulk susceptibility, magnetization, neutron diffraction, and heat capacity measurements. The discovery of the Mossbauer effect in 1958 has lead to an elegant and welcome spectroscopic technique for direct observation microscopic single ion and cooperative magnetic behavior in solids with, of course, iron as an outstanding example. In

this article, we briefly review some of the more salient features of iron-57 Mossbauer spectroscopy as relates to the study of slow paramagnetic relaxation and three-dimensional magnetic ordering of inorganic and organometallic solids having iron atoms as their paramagnetic metal ion centers. Our strategy is as follows. (A) We outline the basic features of magnetic hyperfine splitting (i.e. origins) owing to slow paramagnetic relaxation versus cooperative (three-dimensional) ordering phenomena. (B) Aspects of applied field Mossbauer spectroscopy are then considered. (C) Finally, a number of quite different examples of Mossbauer spectroscopy in the study of ferromagnets or dominant ferromagnetic interactions are presented. Firstly we consider its early application to α-iron, arguably the archetypical ferromagnet. This is followed by a number of more recent examples from this author's and coworker's research. In all that follows, a basic familiarity with Nuclear Gamma Resonance (Mossbauer effect) spectroscopy is assumed. In any event, the reader is directed to a number of important resources[1,2,3] dealing with basic aspects of NGR.

ORIGINS OF NUCLEAR ZEEMAN SPLITTINGS

I. Application of External Magnetic Fields (H_o) to Nuclei in Otherwise Diamagnetic Environments.

This is, of course, the most obvious method for realizing nuclear Zeeman splitting and is of central importance to NMR (rf induced intraspin manifold transitions) via either electromagnets (H_o (max) ~ 3.5 Tesla) or significantly higher values of H_o through the use of superconducting magnets. A primary example of their use is the Nb-Ti solenoid with H_o(max) ~ 9.1 Tesla at 4.2K. On a proton NMR scale, this corresponds to ~ 390 mega Hz. Since iron-57 has significantly smaller nuclear moments[4] ($\mu 1/2 = 0.0906\ \beta_N$, $\mu 3/2 = -0.1539\beta_N$) than the proton ($\mu 1/2 = 2.7927\ \beta_N$) seemingly large values of H_o such as the preceding are not particularly useful in producing spectroscopically resolvable (vis à vis Mossbauer spectra) nuclear Zeeman splittings except in certain special cases to be considered subsequently.

II. Internal Hyperfine Fields Arising from an Atom's Unpaired Electron Spins.

Since the ratio μ(electron)/μ(proton) is ~ 660, it is the atom's own electrons, by far, that have the greatest potential for producing internal hyperfine fields and concomitant large nuclear Zeeman splittings that are readily resolved in typical NGR spectra, of say iron-57. The contributions to the internal hyperfine field are considered in some detail subsequently. Let it be said now that there are two distinct phenomena intimately involving electron spin fluctuations, and magnetic exchange interactions that ultimately lead to very large (static) internal hyperfine fields at NGR nuclei. These are:

(a) Slow Paramagnetic Relaxation. This is basically a single ion effect requiring (a) low T (but not always), (2) dilution of paramagnetic ion centers and (3) zero field splitting of single ion electron spin Zeeman states.

(b) Cooperative (3D) Magnetic Order which requires (1) "low kT" relative to the strength of magnetic exchange interactions, and (2) direct contact or atom-bridged (super) exchange pathways. Factors (1) and (2) lead to the "sudden" development of an internal molecular field (H_n) such that dH_n/dT is usually large near $T_{critical}$ and where H_n results in large resolvable nuclear Zeeman splittings. These can be as large as 60T for high spin Fe^{3+} and are often accompanied by an anomaly in susceptibility (χ_m) vs T, magnetic heat capacity (C_m) vs T, or the observation of "magnetic reflections" in neutron diffraction studies.

III. Effective magnetic fields.

In addition to the sign[5,6] of ΔE (the quadrupole splitting) it is also possible to determine the effective magnetic field (H_{eff}) from perturbed Mossbauer spectra. This is of considerable use in iron coordination chemistry in that H_{eff} may be related to features of electronic structure such as oxidation and spin state as well as degree of covalency and nature of magnetic anisotropy. Measurement of effective magnetic fields also allows determination of the presence or absence of intramolecular

antiferromagnetism in coordination systems that are otherwise magnetically dilute. This aspect will be considered in more detail when a specific exchange-coupled dimeric iron complex is discussed.

In general, the effective magnetic field, H_{eff}, at a Mossbauer nucleus is related to the applied field (H_o) and internal hyperfine field (H_n) by

$$H_{eff} = H_o + H_n \qquad (1)$$

We are interested in spectra of quadrupole split diamagnetic and rapidly relaxing paramagnetic systems as well as the cases of slow relaxation and pure Zeeman interaction which are considered first. The following situations arise where ΔE is the quadrupole splitting.

(a) $\Delta E = 0$, $H_n \neq 0$. In this instance, the characteristic six-line pure Zeeman pattern (Figure 1(a),(b)) of a magnetically ordered iron system is observed. A similar spectrum is also observed for a slowly relaxing paramagnet in the limit of infinitely long relaxation time between the components of its Kramers' doublets. The spectra correspond to the normally allowed transitions ($\Delta M_I = 0, \pm 1$) among the magnetically split $I = 1/2$ ground and $I = 3/2$ excited states with magnetic field relaxation time long relative to the nuclear Larmor precession frequency. The growth of such spectra (in $H_o = 0$) as a function of decreasing T is shown in several examples (vide infra).

(b) $\Delta E = 0$, $H_n = 0$, $H_o \neq 0$ and parallel to the γ-ray. This situation corresponds to an effective magnetic field equal to the applied, as in the case of a diamagnet or a rapidly relaxing paramagnet whose metal ions are in sites of cubic symmetry in the limit of large H_o. The result is the spectrum of Figure 1(c). One sees that transitions 2 and 5 vanish owing to their $\sin^2 \theta$ dependence.[3] The angle θ between the direction of γ-ray propagation and H_o is zero for a longitudinally (axially) applied field. The energy separation of transitions 1-6 is $3\alpha + \beta$ and is, of course, proportional to the applied field. The quantities $\alpha = g_{3/2}\beta_N H$ and $\beta = g_{1/2}\beta_N H$ where $g_{3/2}$ and $g_{1/2}$ are the excited and ground state gyromagnetic ratios and β_N is the nuclear magneton. For iron-57, the ratio $\beta/\alpha = g_{1/2}/g_{3/2}$ has been determined[4] using Mossbauer spectroscopy and has the value -1.715. The

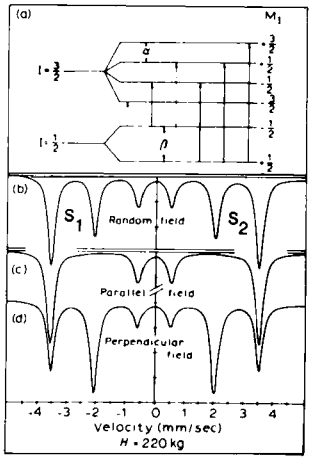

Figure 1. Pure Zeeman Splitting.

ground state gyromagnetic ratio has been measured[7] independently using NMR and is 0.1828. Thus with the preceding values of α, β etc. and a known applied field, the total splitting $3\alpha + \beta$ is determined. In the case of the standard Mossbauer calibrant α-iron, the splitting is 10.626 mm/sec, corresponding to H_n = 330 kGauss. These numbers correspond to the saturated ferromagnetic state at ambient temperature. Single-line (ΔE = 0) diamagnetic absorbers such as $K_4Fe(CN)_6$ and TiFe alloy[8] also exhibit spectra such as that illustrated in Figure 1(c) in large external (axial) fields.

(c) $\Delta E = 0$, $H_n = 0$, $H_o \neq 0$ and perpendicular to the γ-ray. The comments for this case are similar to those for case (2), except that transitions 2 and 5 are intensified relative to 1, 3, 4, and 6 which are all expected to be weaker from their $1+\cos^2$ dependence[3] (Figure 1(d)).

(d) Combined Nuclear Zeeman and Quadrupole Splitting, $H_n \neq 0$, $E \neq 0$, $H_o = 0$

The spectrum in this case is like that of Figure 1(a) except that the center of the inner four transitions is shifted toward lower or higher energy relative to the center of transitions 1 and 6 because of the non-zero quadrupole interaction. For axial symmetry this shift may be related to the angle Θ between H_n and the principal axis of V_{zz} (the principal component of the electric field gradient tensor) by the relation[3]:

$$S_1 - S_2 = -\Delta E(3\cos^2\theta - 1) \qquad (2)$$

where S_1 is the separation of transitions 1 and 2 and S_2 that of transitions 5 and 6, and ΔE is the quadrupole splitting determined from the paramagnetic phase. Thus for pure Zeeman splitting, as in Figures 1(a)-(d), $S_1-S_2 = 0$ and a symmetric pattern is evident.

IV. Contributions to the internal hyperfine field (H_n)

The large internal hyperfine fields exerted on the nuclei of atoms in exchanged-coupled cooperatively-ordered or slowly-relaxing systems ultimately arise from the paramagnetism of the atom's electrons and can be divided into three components:[3]

(a) $H_S \propto (\psi_\uparrow(0)^2 - \psi\downarrow(0)^2)$ (the Fermi contact term);

(b) $H_L \propto \langle r^{-3} \rangle \langle L_z \rangle$ or $H_L \alpha \langle r^{-3}\rangle(g-2)\langle S_z\rangle$ (the orbital moment contribution) and

(c) $H_D \propto \langle r^{-3} \rangle \langle 3\cos^2\theta - 1\rangle\langle S_z\rangle$ or alternatively $H_D \propto V_{zz}/e\langle S_z\rangle$ (the dipolar interaction).

Thus, $H_{eff} = H_o + H_n = H_o + H_s + H_L + H_D$. It is seen that (1) is the result of an imbalance of "s" electron α and β spin density at the nucleus. This imbalance results from the polarization caused by the differential interaction of "s"(α) and "s"(β) with unpaired valence shell "d" and "f" electrons. On the other hand, (2) is directly related to the magnitude of orbital angular momentum (L) for a particular unpaired valence shell electron of radius r. It is clear that (3) is operative only for sites of less than cubic symmetry and is the result of a through space interaction of the valence shell spin angular momentum with that of the nucleus. The terms H_L and H_D can either oppose or add to H_S. For the case of iron, H_S is ~ 11T/unpaired electron (1T = 10 kiloGauss). Thus for high spin iron III, ^6A ground term, in cubic symmetry where L, H_L, and H_D are all ~ 0, limiting low temperature values of H_n ranging between 40 to 60T can be observed. For high spin iron II, somewhat smaller values of H_n (to ~ 35T) are observed owing to a combination of the smaller value of <S>, namely two, and the possibility of an orbital contribution, H_L that generally opposes H_S. Reduction of H_n for any oxidation state is also related to variable covalency and delocalization effects depending on the ligands. This can lead directly

to delocalization of metal ion "S" spin density and an increase of $\langle r^3 \rangle$ for the valence shell electrons. These are effects that result in a decrease of any of H_S, H_L or H_D in view of their respective equations. An additional effect leading to substantially reduced values of H_n is the so-called "zero point spin reduction" present in certain low dimensional magnetic systems.[9]

V. Single Ion Zero Field Splitting and Slow Paramagnetic Relaxation versus Cooperative Three Dimensional Order.

Slow paramagnetic relaxation-hyperfine splitting is a dynamic single ion effect resulting in part from the zero field splitting of the ground (electronic) spin manifold. This is shown in Figure 2 for the

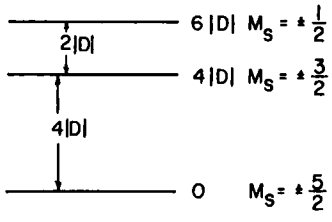

Figure 2. Negative axial zero field splitting for high spin Fe(III)

spin sextet of high-spin iron III. Since this is a Kramers ion, the ground state of the zfs ion must be the doubly degenerate $M_S = \pm 1/2$ ($D>0$) or $M_S = \pm 5/2$ ($D<0$) in zero applied magnetic field. Relaxation in the former is rapid while that in the latter as well as $M_S = \pm 3/2$ is slow. We will consider only the case of high spin iron III with D large and negative and at low temperatures. In this situation, the dominant relaxation mechanism is spin-spin relaxation (interatom exchange of S_z values) as opposed to spin-lattice that is more important to $L \neq 0$ ions such as high spin Fe^{2+}. If the metal ions are closely situated so as to allow for rapid interatom spin flips via direct dipolar interactions (but not close enough for direct magnetic exchange or superexchange) there will be no spectral broadening even though a "slowly" relaxing ($M_S = \pm 5/2$) doublet is being populated. However, dilution[10] of the metal ions to distances typically ≥ 7.5 Å (for high -spin FeIII) leads to longer spin-spin relaxation times whose reciprocal corresponds to a

dynamic, temperature dependent frequency that eventually becomes comparable to the Larmor precession frequency of the nuclear moment.[11] This leads to the gradual development of a non-zero time averaged value of H_n and gradual Zeeman splitting of the Mossbauer spectrum as the $M_S = \pm 5/2$ doublet is progressively populated. One observes a single six line pattern in the limit of low T since the $M_S = \pm 3/2$ at 4D is little populated when D is large.

The limiting (zero field) low temperature spectra corresponding to three dimensional magnetic ordering processes (antiferromagnetism, ferro- and ferrimagnetism) are generally identical in appearance to those for slow relaxation. The difference is that H_n at the individual metal ion sites now corresponds to and is generally thought of as collinear with a spontaneous magnetization developing in the bulk sample. The latter originates from exchange interactions (either direct e.g. α-Fe, or super-exchange e.g. α-Fe_2O_3) between the metal ions that become comparable to or greater than the thermal spin randomization effects as the temperature is decreased and a molecular exchange field develops. In general and in contrast to slow relaxation, the hyperfine splitting process occurs "suddenly" over a small temperature interval reflecting the cooperative (usually second order) phase transformation nature of magnetic ordering. In addition, the internal hyperfine field is very temperature dependent in the vicinity of $T_{critical}$ and only levels off as magnetic saturation is reached at low temperatures, often as $T \longrightarrow 0°K$.

The Néel or Curie temperature as measured via extrapolation of $H_n \longrightarrow 0$ is usually in reasonable agreement with susceptibility results. Actually, at values for critical temperatures as determined by more precise methods such as classical measurements of the temperature dependence of magnetic heat capacity, Mossbauer spectra sometimes exhibit a substantial non-zero value of H_n. This problem is not dealt with here. The dimensionality of magnetic order (1, 2, or 3) is related to the so-called "critical exponent" which can be determined from fits to functions such as:

$$H_n(T)/H_n(0°K) = B(T_c - T)^{\beta}/T_c \qquad (3)$$

in temperature ranges as close as feasible to $(T_c-T) = 0$ where β is the critical exponent. It should be mentioned that hyperfine splitting and ordering may not be sharp but can actually be spread over larger temperature intervals as exemplified in finely divided superparamagnetic materials or highly defect structures. Rather characteristic Mossbauer spectra are observed in these cases. Finally, no hyperfine splitting may occur even though other techniques give clear evidence of magnetic order. This is rare but can occur when the various contributions to H_n, namely H_S, H_L, H_D fortuitously cancel e.g. as for the case of anhydrous ferrous chloride for which magnetic susceptibility studies clearly indicate $T_{Néel} = 23$ K.

VI. Intensities - Single Crystal Studies

So far, all of the discussion has referred to the Mossbauer spectra of isotropic, polycrystalline powders or powders whose paramagnetic moments are polarized to the direction of an applied field, H_o. We now focus on oriented single crystals in zero and non-zero magnetic fields. For convenience throughout the rest of this section, should a field be applied, it will either be longitudinal (axial) i.e. parallel to the direction of gamma ray propagation, $E\gamma$ or transverse i.e. perpendicular to $E\gamma$. The orientation will then refer to the angle (θ) between the easy axis or plane of magnetization and $E\gamma$ for a three dimensionally ordered material. Hopefully, the foregoing axes will be collinear with a convenient laboratory crystallographic axis of a favorable unit cell, e.g. orthorhombic or tetragonal. As with other spectroscopies, the utility of the Mossbauer effect is significantly enhanced when applied to single crystal samples and this will be seen for the example of Fe_2O_3.[12] In addition, one can also determine polarized[13] gamma ray Mossbauer spectra for single crystal samples through the use of a polarized, magnetically ordered gamma ray source, e.g. a magnetic α-Fe foil matrix onto which Co^{57} activity has been electroplated and then subsequently annealed to the interior. (The I = 5/2 precursor nuclear spin level ultimately leading to the 14.4 kev I = 3/2 Mossbauer excited gamma ray level of iron-57 is populated by the electron capture decay of Co^{57}: $Co^{57} + e^- \longrightarrow Fe^{57}$. In any event the subject of polarized NGR spectra is beyond the scope of the present article.

For the transitions of the polycrystalline powder form of a 3D-ordered ferro- or antiferro-magnet and thus a random orientation of magnetic domains in zero applied field, one expects the familiar 3:2:1:1:2:3 pattern of integrated intensity as in Figure 1b. Otherwise for $E\gamma$ parallel or perpendicular to an easy axis (or plane) of magnetization (H_o again equal to zero) one sees 3:0:1:1:0:3 (Figure 1c) or 3:4:1:1:4:3 (Figure 1d) respectively. The $\Delta M_I = \pm 2$ transitions are normally forbidden or of very low intensity and are not considered further herein. The application of these results in obtaining useful correlations for a number of specific examples is considered subsequently.

VII. High Field Mossbauer Spectra of Ordered Systems and Determination of The Three Dimensional Ground State.

(a) Antiferromagnets. We shall now show how the determination of Mossbauer spectra in external fields can aid in distinguishing type of magnetic order present, i.e. the nature of the 3D-ordered ground state, even for polycrystalline samples. Probably the simplest type of antiferromagnet is the two sublattice collinear Néel magnet in which the magnetization and internal hyperfine field of one sublattice $H_n(\alpha)$ is antiparallel to and exactly opposes that of the other $H_n(\beta)$. For a random polycrystalline powder form of such a uniaxial antiferromagnet at $T < T_N$, one expects little if any effect from an applied field (H_o) on its Mossbauer spectrum. That is, for a thin absorber, an approximate 3:2:1:1:2:3 intensity pattern in maintained and the average effective Zeeman-splitting (H_{eff}) is unchanged, where $H_{eff} = H_o + H_n$. One simply observes transition broadening owing to the distribution of angles of sublattice magnetizations with respect to H_o. The preceding is the case provided H_o is less than H_{sf}, the so-called spin-flop field field at which a first order phase transformation corresponding to the flopping of the spins to a direction normal to H_o occurs. The appropriate phase diagrams are shown in Figure 3. Note that for the single crystal form of the uniaxial (collinear Néel) antiferromagnet, α-Fe_2O_3, in zero field or in a longitudinal field such that $H_o < H_{sf}$ and applied along the easy axis, the $\Delta M_I = 0$ transitions have zero intensity, i.e. a 3:0:1:1:0:3 pattern is observed (Figure 4). H_o is parallel to the opposing sublattice magnetic hyperfine fields, $H_n(\alpha)$, and $H_n(\beta)$. Thus the highest and

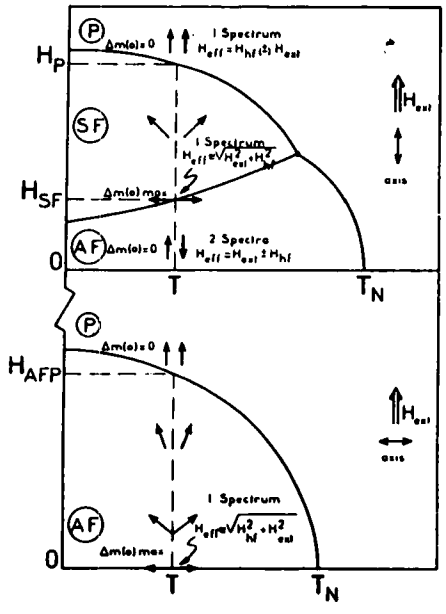

Figure 3. Phase Diagrams for a Uniaxial Antiferromagnet.

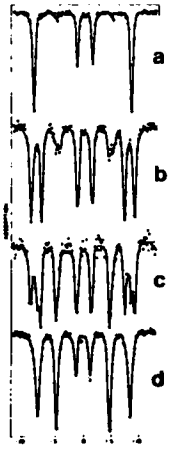

Figure 4. Spectra of Single Crystal αFe_2O_3 at 4.2 K with $H_o = 0$; b) $H_o = 65$ KOe; c) $H_o = 66$ KOe; d) $H_o = 70$ KOe.

lowest velocity transitions of the spectrum are normally observed to be split into symmetric doublets corresponding to the addition of H_o to one of the antiferromagnetic sublattices, say $H_n(\alpha)$ and subtraction of H_o from the other, $H_n(\beta)$ (Figure 4b). For $H_o \geq H_{sf}$, the foregoing splitting vanishes and the intensity pattern changes to 3:4:1:1:4:3 in accord with the angular components of the selection rules for $\theta = 90$ (Figure 4d for single crystal α-Fe_2O_3). Note that only one (six line) spectrum is now observed since at the stage of Figure 4, $H_o > H_{sf}$. We are "well into" the spin-flop phase where H_n is perpendicular to both $H_n(\alpha)$ and $H_n(\beta)$. From 4b, it is evident that spin flopping has already occured in some portions of the single crystal. In addition, Figure 4b shows that the transitions just above and below zero velocity have broadened considerably relative to 4a ($H_o = 0$) but are not observed to split into doublets. Clearly the energies of the inner $\Delta M_I = \pm 1$ transitions are not as sensitive to H_o as the outer $\Delta M_I = \pm 1$ transitions. The continuous second order antiferro to "paramagnetic" phase transition of a uniaxial antiferromaget (bottom of Figure 3) can also be observed when H_o is perpendicular to the easy axis. It is clear that the entire H vs. T phase diagram of an ordered antiferromagnet can be mapped using

Mossbauer spectroscopy. This has been done for the single crystal forms of metamagnetics such as $FeCl_2 \cdot 2H_2O$, $FeCl_2$ and more complex systems such as spiral spin structures, e.g. $FeCl_3$.[13]

(b) 3D-Ferromagnets. Three dimensional ferromagnets are decidedly rarer than antiferromagnets. Nevertheless, they are fundamentally less complex than the latter in that they can be generally viewed as single lattice systems with all spins parallel. There is typically a very large susceptibility even at temperatures slightly above T_{Curie}. Thus, unlike antiferromagnets, relatively small values of H_o lead to substantial magnetization and effective internal fields just above T_{Curie} (vide infra). Ferromagnets also exhibit rather characteristic high field Mossbauer spectra below T_{Curie}. Relatively small axial fields lead to ready polarization for polycrystalline powders, foils, or unoriented single crystals and domain alignment parallel to H_o and E_γ. Thus one observes 3:0:1:1:0:3 spectral patterns reminiscent of Figures 1c for axially applied external fields. However, in contradistinction to an antiferromagnet with H_o parallel, the easy axis, one never sees more than four transitions since there is only one magnetic lattice, namely the field oriented and now extensive domain of parallel spins.

For later reference, we conclude this section by mentioning the obvious but important fact that transverse applied fields ($H_o(1)$) generally have the opposite effect of that produced via longitudinal fields ($H_o(11)$). Thus the spin flop transition of an antiferromagnet will correspond to diminution of the ΔM_I transitions. In the case of a ferromagnet, $H_o(11)$ leads diminution of the $\Delta M_I = 0$ transition while $H_o(\ )$ results in enhancement.

APPLICATIONS TO FERROMAGNETIC MATERIALS

The primary thrust of this symposium is the properties of high-spin and ferromagnetic materials. Hence, we conclude this article with

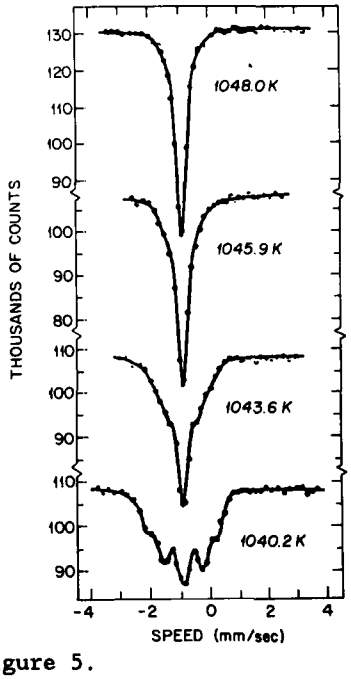

Figure 5.
Temperature dependence of the Mossbauer spectrum of (Fe-57) isotopically enriched iron metal foil in the immediate vicinity of T(Curie) ~ 1045 K (with permission from Ref. 4).

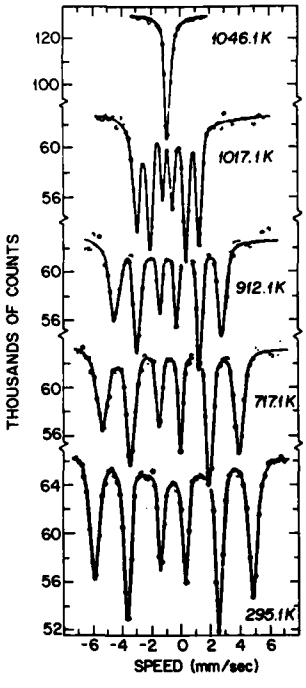

Figure 6.
Temperature dependence of the Mossbauer spectrum of (Fe-57) isotopically enriched iron metal foil from above T(Curie) to ambient temperature (with permission from Ref. 4).

several applications of nuclear gamma resonance spectroscopy to materials having dominant ferromagnetic exchange interactions.

I. Strong Ferromagnetic Interaction (α-Fe)

Zero field Mossbauer spectra illustrating the magnetic ordering of metallic iron are shown in Figures 5 and 6. In this work[4], absorbers were foils ~ 0.001 inch thick and enriched with iron-57 from normal abundance (~2.2%) to 53.6% thus leading to line broadening. The rapid

growth of a molecular field is evident with H_n = 33T at ambient temperature. Thus the material is essentially saturated since H_n (4.2K) = 33.8T. The Curie temperature, T_c, is found to be 1045K (~772C) in excellent agreement with determinations (770C) via other methods. The ferromagnetism of this material is consistent with high field spectra determined by this author and shown in Figure 7 for a thin (0.2 mil) natural abundance iron metal foil absorber. The near 3:2:1:1:2:3 intensity pattern for the spectrum at 293K (Figure 7-top) corresponds to an essentially random array of ferromagnetic domains relative to E_γ . On the other hand, spectrum at the bottom of Figure 6 indicates significant magnetization (in H_o = 0) in the plane of the foil, i.e. normal to E_γ .

In ΔM_I = 0 transitions (arrows-Figure 7) have all but disappeared at H_o = 2.5T. This is consistant with a ferromagnetic ground state such

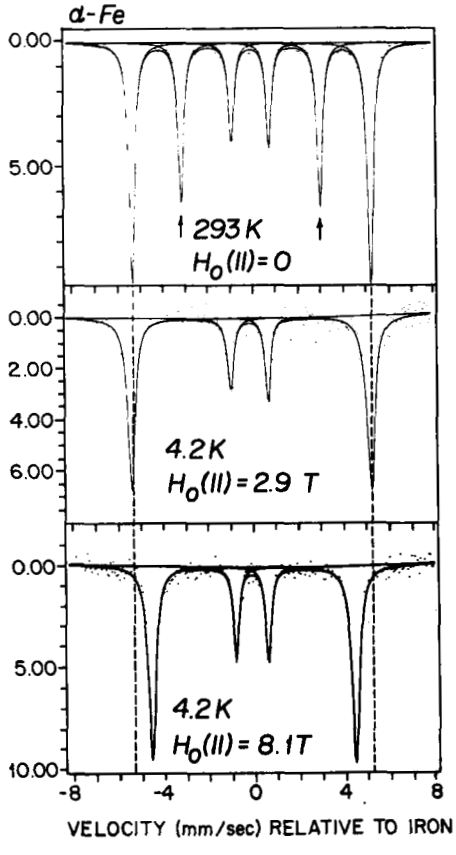

Figure 7. Some high field Mossbauer spectra for natural abundance (Fe-57) iron foil, (W.M. Reiff previously unpublished data).

that the domains are polarized parallel to H_o and therefore E_γ . That it typically requires an H_o value varying from 2 to 3T to fully polarize a given foil's moments is the result of a combination of the operation of an opposing demagnetizing field (~2.2T for α-Fe) and expenditure of energy to overcome the anisotropy energy associated with ferromagnetic domain rotation and boundary movement. Finally (after complete magnetization), the overall splitting of the spectrum at the bottom of Figure 7 indicates a decrease of effective internal field relative to H_o = 0. This results from the fact that the primary contribution to the internal hyperfine field, (H Fermi-contact) is negative relative to H_o.

II. Weak Ferromagnetic Interactions - Ionic Fluorides of High Spin Fe(III)

We now go from the very strong (direct) magnetic exchange of α-Fe to weak super-exchange exhibited in ionic fluorides of high-spin iron III and recently studied by this author. The exchange involves close contacts of delocalized spin density between $[FeF_6]^{3-}$ or $[FeF_5 \cdot H_2O]^{2-}$ polyhedra via hydrogen bonds or lithia bridging.

(1) $K_2FeF_5 \cdot H_2O$

The structure of this material is shown in Figure 8 while pertinent Mossbauer spectra are given in Figure 9. Clearly, $K_2FeF_5 \cdot H_2O$ is

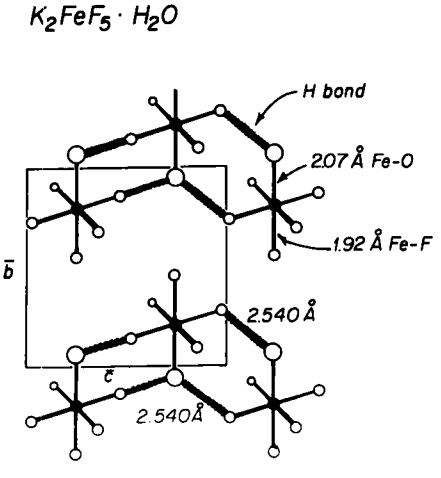

Figure 8.
Local structure and hydrogen bonding of $K_2FeF_5 \cdot H_2O$.

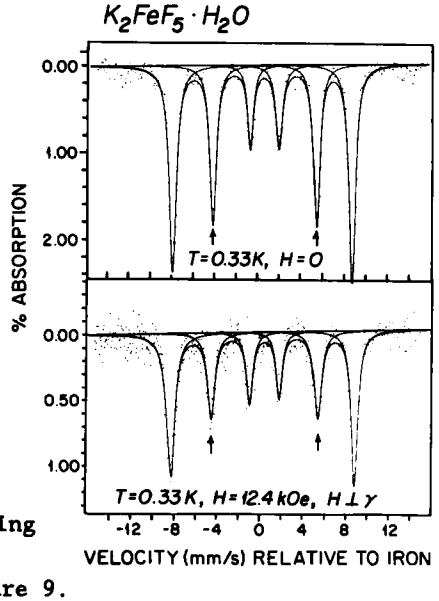

Figure 9.
Sample spectra for $K_2FeF_5 \cdot H_2O$ in the He-3 range.

ordered and exhibits a low field spin-flop in a transverse field of ~ 1 T for $T < T_N$ (0.9 K). (Note: diminution of the $\Delta M_I = 0$ transitions). This agrees with a 3D-AF ground state suggested by a susceptibility study.[14] Above T_N, the field dependence is quite different and suggests the possibility of substantial 1D-antiferromagnetic correlation.

(2) β-Li_3FeF_6

We have found[15] that β-Li_3FeF_6 orders near 1.15 K as shown via zero field Mossbauer spectroscopy. The preliminary susceptibility data (squid results at H_o = 30 to 2 K; not shown) suggest some type of ferromagnetic behavior (θ = + 1 K and a very rapid rise in moment) although we do not reach T_{Curie} by the susceptibility route. Clearly more detailed susceptibility study is necessary. In any event, the transverse field spectra at 0.51 K (Figure 10) and 0.33 K (not shown) -- i.e. well below T_{Curie} -- show clear polarization of the sample moments (for a random powder sample) perpendicular to the direction of γ-ray propaga-

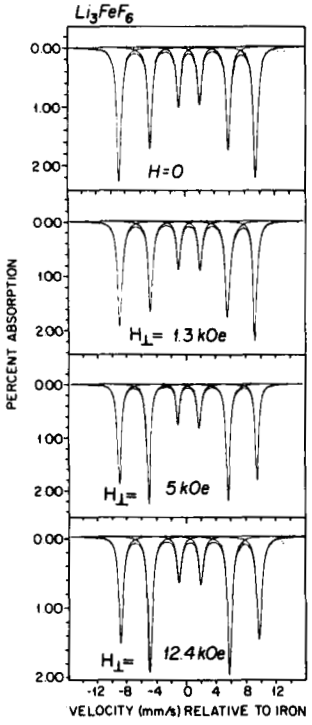

Figure 10. Sample spectra for β-Li_3FeF_6 in the He-3 range.

tion fully consistent with a 3D-ferromagnetic ground state. (Note: Enhancement of the $\Delta M_I = 0$ transitions). This behavior is not only unexpected but the exchange interactions are surprisingly strong relative to, say, $K_2FeF_5 \cdot H_2O$ which has hydrogen bonding (Figure 8). The magnetic exchange in β-$Li_3[FeF_6]$ is likely transmitted (and apparently efficiently) through LiF_4 tetrahedra (2/9 of the total Li) that bridge the ferric octahedra.[16] It might be expected that α-$Li_3[FeF_6]$ orders at a somewhat lower temperature in view of its ferric ion bridging entirely via LiF_6 octahedra implying weaker individual Li-F bonds. Additional, detailed studies of both the α and β forms of Li_3FeF_6 are in progress.

III. A 1D-Ising Ferromagnet

We now briefly turn to $[(CH_3)_3NH]FeCl_3 \cdot 2H_2O$, hereafter FeTAC[17], a one dimensional Ising chain ferromagnet pictured in Figure 11. The

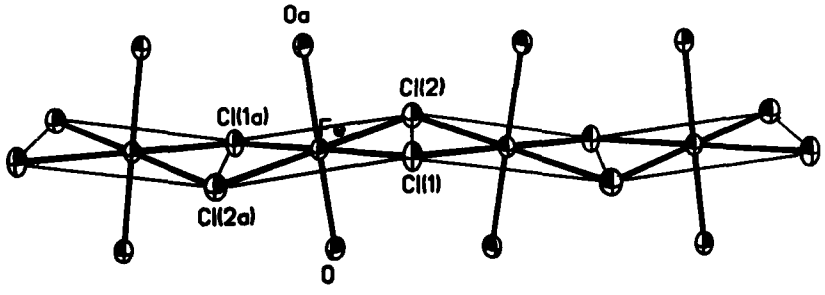

Figure 11. Articulation of the trans$\{FeCl_4(H_2O)_2\}$ unit in the chain structure of $[(CH_3)_3N]FeCl_3 \cdot 2H_2O$ (FeTAC).

intrachain ferromagnetic exchange is large ($J/k_b \approx +17$ K). A substantially weaker (antiferromagnetic) interchain exchange leads to 3D order at ~ 3.1 K. The chains as pictured are diluted by uncoordinated lattice chloride anions and tri-methylammonium cations. Magnetization measurements show the material to be metamagnetic with H_o(critical) ~ 90 Oe.

Some Mossbauer spectra (polycrystal sample) showing the three-dimensional magnetic ordering of FeTAC are given in Figure 12. There is an abrupt transition to a three-dimensionally ordered state just below 3.2 K, in quite good agreement with the magnetic susceptibility measurements. The spectrum at 3.5 K shows initial broadening above the temperature of ordering as indicated by susceptibility. It is possible that this broadening is the result of single ion slow paramagnetic relaxation phenomena -- that is, a negative zero field splitting of the

single ion spin quintet manifold leading to a slowly relaxing $m_s = \pm 2$ ground Kramers doublet. Such broadening can also be the result of soliton effects (moving domain boundaries in the present context) in a one-dimensional magnet just above the critical ordering temperature.[18]

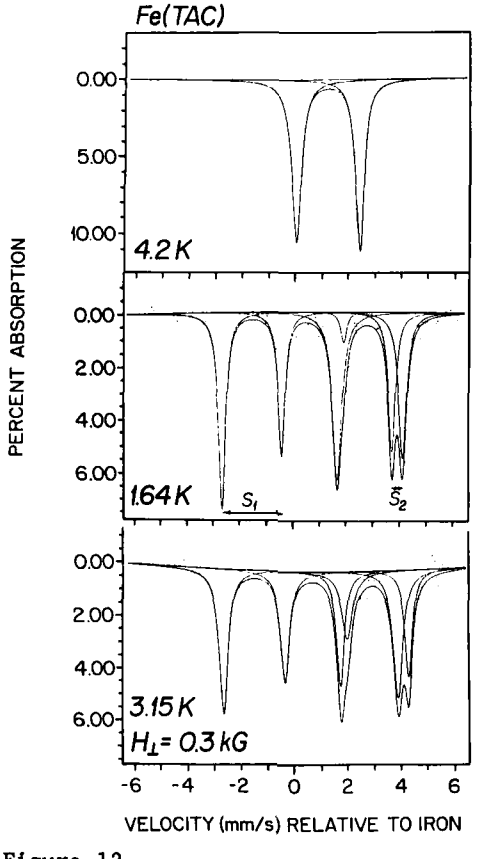

Figure 12.
Mossbauer spectra of FeTAC, top (3.5 K, $H_o = 0$), middle (1.64 K, $H_o = 0$), bottom (3.15 K, $H_o = 300$ Oe).

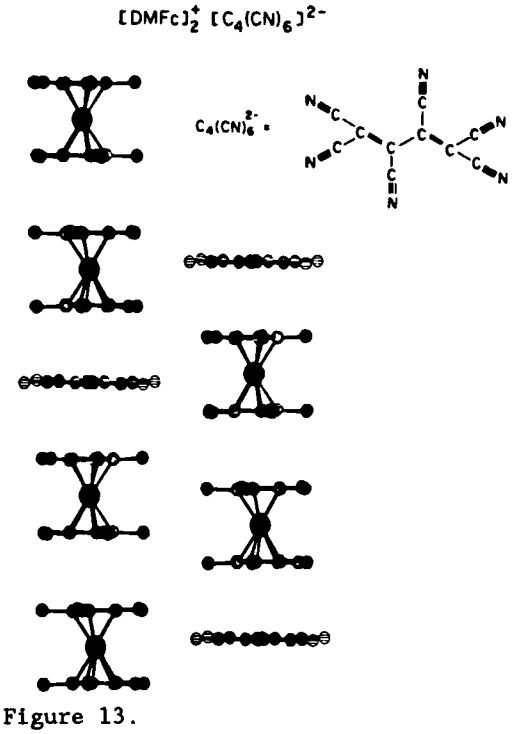

Figure 13.
Schematic of the 2:1 charge transfer polymer $[DMFC]_2^+[C_4(CN)_6]^{2-}$.

FeTAC readily magnetizes on application of very small fields betraying the strong ferromagnetic nature of its intrachain exchange. This is seen in the spectrum at 3.15 K in a transverse applied field of only 300 Oe (bottom of Figure 12). The resulting spectrum has a value

of internal hyperfine field and degree of resolution and magnetic saturation that are comparable to the zero field spectrum taken at 1.64 K, $H_{internal}$ = 20T (middle of Figure 12). The limiting spectrum at 1.64 K gives clear evidence of a large quadrupolar shift (vide infra) and perturbation of the hyperfine split spectrum; in fact the spectrum is reminiscent of many ferrous systems[19,20] in which eight transitions are actually present ($\Delta M_I = \pm 2$ transitions weakly allowed).

IV. Ferromagnetically Coupled Dimers

We conclude with some observations for some new 2:1 cation:polycyanide dianion phases[21] whose charge transfer polymer structure is shown in Figure 13 for the example of $[DMeFc]_2^+[C_4(CN_6)]^{2-}$. The material contains a dianionic polycyanide species. The temperature dependence of its Mossbauer spectra is clearly unprecedented and to our knowledge, is the first example in which hyperfine splitting grows, reaches a maximum intensity and then, with further decreasing temperature, totally vanishes.

$[DMeFc]_2^+[C_4(CN)_6]^{2-}$ as is pictured in Figure 13, corresponds to parallel chains of pairs of DecaMethylFerroCenium cations alternating with single $C_4(CN)_6^{2-}$ anions. Its characteristic singlet Fe-57 Mossbauer spectrum at 300 K (Figure 14, top) incontrovertably confirms the fact that all iron is present as low-spin Fe(III), i.e. decamethylferrocenium cations (ferrocene and decamethylferrocene formally contain iron(II) and always exhibit well resolved quadrupole doublet spectra ΔE > 2mm/sec). Thus from electrical neutrality considerations and the 2:1 stoichiometry confirmed by x-ray structure determinations, the hexacyanobutadiene moiety must be present as a dianionic species, $C_4(CN)_6^{2-}$.

The Mossbauer spectra that we now present strongly suggest unusual dynamic behavior and the presence of a novel triplet species in $[DMeFc]_2^+[C_4(CN)_6]^{2-}$ for ferromagnetically coupled dimeric cation pairs. Sample spectra are shown in Figures 14 and 15. On gradual cooling, slow paramagnetic relaxation-broadening and hyperfine splitting develop with maximum intensity and resolution for the hyperfine background occurring at ~ 10 K. However, and to our surprise, below this temperature the strong central singlet of the rapidly relaxing paramagnetic phase begins

to grow again until a singlet reminiscent of 300 K is all that remains at 0.53 K. Closer examination of the spectra in the vicinity of ~ 25 K shows the emergence of two hyperfine patterns suggesting either iron site inequivalence perhaps resulting from a Jahn-Teller distortion or other phase transformation in this temperature region. Another and more likely possibility is that there is a *unique iron(III) environment*; however, multiple Zeeman splitting patterns are observed as the result of highly anisotropic magnetic hyperfine interactions. We emphasize that the observed behavior has been reproduced and is entirely reversible. In addition, it is also found for other dianion species such as $C_6(CN)_6^{2-}$ and iso-$C_4(CN)_6^{2-}$ as well as the s = 0 Co(III) diluted

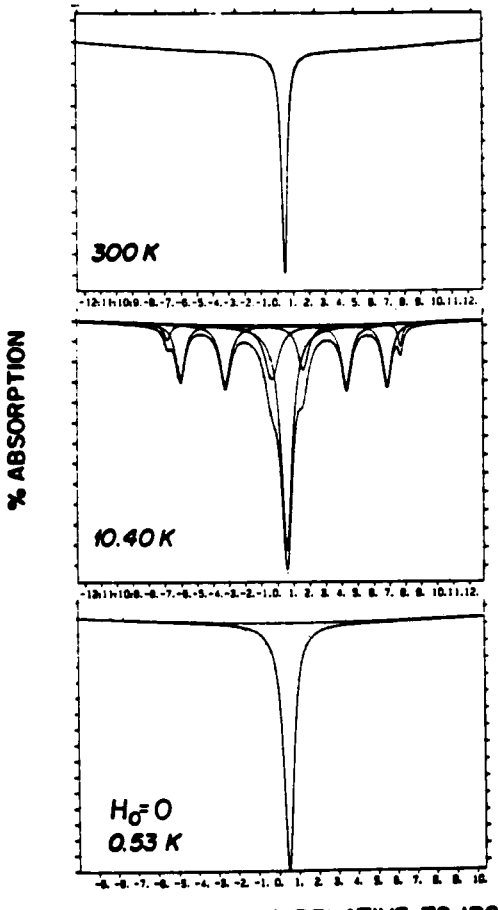

Figure 14.
Sample spectra showing the growth and vanishing of hyperfine splitting for $[DMeFc]_2^+[C_4(CN)_6]^{2-}$.

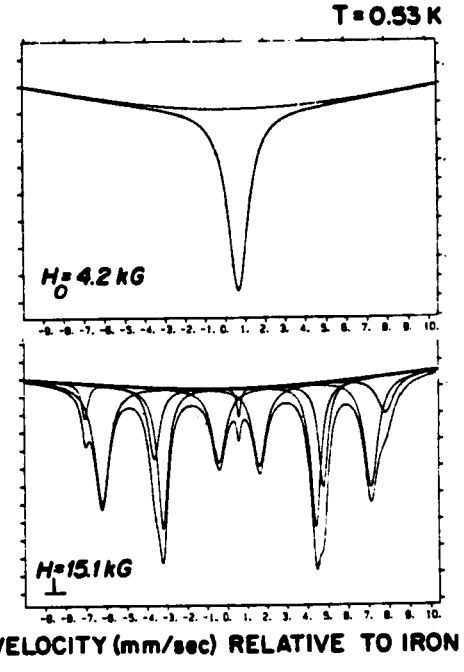

Figure 15.
Some transverse field spectra for $[DMFC]_2^+[C_4(CN)_6]^{2-}$ at 0.53 K.

analogs. The "inequivalence" (not resolved in the broadened singlet at 0.53 K; compare the tops of Figures 14 and 15) is clearly resolved again in a *transverse applied field* spectrum at 0.53 K as shown in Figure 15, bottom. The limiting gross intensity pattern (H_o = 15.1 kG) is exactly as predicted for a rapidly relaxing paramagnet or diamagnet whose sites have been induced to slowly relax by the applied field and polarized so that their magnetization is perpendicular to the direction of gamma ray propagation. The susceptibility of the present 2:1 system has been measured at 30 G, 300 G and 3000 G with the same result, "simple" paramagnetism but very non-Curie-Weiss behavior. We observe no maximum in the temperature dependence of the magnetic susceptibility for any value of applied field to as low as 30 G.

The explanation of our observations for the 2:1 cation:dianion phases is suggested by the structure of these systems, i.e. one containing cation pairs (Figure 13). At sufficiently low temperatures, such pairs can act as magnetic exchange coupled dimers. The "magnetic" literature is full of such s = 1/2, s = 1/2 dimers, particularly s_{total} = 0 (singlet) ground state antiferromagnetically coupled dimers of

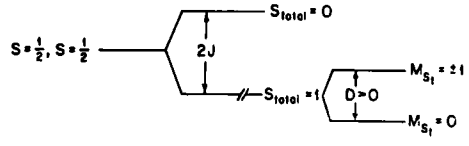

Figure 16. Ferromagnetic coupling and axial zero field splitting for s = 1/2 pairs.

Cu(II). For such AF dimers, a maximum in the temperature dependence of the magnetic susceptibility (χ_m) is typically observed and is theoretically predicted. The exchange interaction J is negative with the singlet-triplet separation being 2 J. These are, however, well characterized examples of s_{total} = 1 ground state (J > 0) ferromagnetically coupled dimers for which a simplified (spin only) energy level diagram is given in Figure 16. This is undoubtedly the case for the present $[DMFC]_2^+$ pairs. Such a dimer's s_{total} = 1 (nominal) ground state can be (positive) zero field split to an excited $m_{s(total)} = \pm 1$ and a true $m_{s(total)}$ = 0 ground state, as shown on the right side of Figure 16.

Large zero-field splittings of this type can result from the highly anisotropic magnetic exchange operative in these systems. Decreasing the temperature for such a system would then initially lead to population of the slowly relaxing $m_{s(total)} = \pm 1$ (since $\Delta m_{s(total)} = \pm 2$ electronic transitions are highly forbidden) and hyperfine splitting via slow (intra and inter) dimer paramagnetic relaxation. Ultimately exclusive population of the nonmagnetic $m_{s(total)} = 0$ ground state would occur at very low T. Concommitant with the latter would be the vanishing of all hyperfine splitting effects as observed. *Finally, and consistent with our observations, J positive dimers are not expected to exhibit a maximum in* χ_m. This system and the related $[DMeFc]_2^+[C_6(CN)_6]^{2-}$ (where $C_6(CN)_6^{2-}$ = hexacyanotrimethylene cyclopropane) are clearly worthy of further detailed study. Such study is currently underway in a fruitful, continued collaboration with Dr. Joel S. Miller and colleagues of E.I. du Pont de Nemours and Co., Inc. Co., C.R.&D., Wilmington, DE. In particular, we are performing detailed fits to the temperature dependence of the susceptibility using the Bleaney-Bowers equation to arrive at J (intra-dimer). We hope to determine D values via study of the temperature dependence of heat capacity for $(DMeFc)_2^+C_6(CN)_6^{2-}$ and the corresponding isomorphous diamagnetic cobalticinium analog. A Schottky anomaly should be evident in C versus T after subtraction of the lattice contribution.

Acknowledgments

The author is pleased to thank Dr. Joel S. Miller for the invitation to the present symposium. He also wishes to acknowledge his collaboration with Dr. Chris Landee (Clark University) on the study of FeTAC and Dr. Jian Hua Zhang, perhaps his most productive recent graduate student. Finally the recent past support of the NSF-DMR Solid State Chemistry Program is continually appreciated.

REFERENCES

1. V. I. Goldanskii and R. H. Herber (Eds.), Chemical Application of Mossbauer Spectroscopy, Academic Press, New York, 1968.
2. G. K. Wertheim, Mossbauer Effect: Principles and Applications, Academic Press, New York, 1964.
3. N. N. Greenwood and T. C. Gibb, "Mossbauer Spectroscopy," Chapman and Hall, Ltd., London, 1971.
4. R. S. Preston, S. S. Hanna, J. Heberle, Phys. Rev., 128 (1962) p. 2207.
5. W. M. Reiff, Coord. Chem. Rev. 10, (1973) p. 37.
6. R. L. Collins, J. Chem. Phys., 42 (1965) p. 1072.
7. G. W. Ludwig and H. H. Woodbury, Phys. Rev., 117 (1960) p. 1286.
8. L. J. Swartzendruber and L. H. Bennett, J. Res. Nat. Bur. Stand., Sect. A, 74 (1970) p. 691.
9. C. E. Johnson, "Proceedings of the International Conference on the Applications of the Mossbauer Effect," Jaipur, India (1981) p. 72.
10. J. W. G. Wignall, J. Chem. Phys., 44 (1966) p. 2462.
11. H. H. Wickman and G. K. Wertheim, "Spin Relaxation in Solids and After Effects of Nuclear Transformations" in Chemical Applications of Mossbauer Spectroscopy, V. I. Goldanskii and R. H. Herber (Eds.), Academic Press, New York, 1968.
12. G. J. Perlow, S. S. Hanna, M. Hamermesh, C. Littlejohn, D. H. Vincent, R. S. Preston and S. Heberle, Phys. Rev. Letters, 4 1960) p. 74.
13. R. B. Frankel, "Mossbauer Effect Methodology," 9 (1974) p. 151 and references therein.
14. R. L. Carlin, R. Burriel, J. A. Rojo and F. Palacio, Inorg. Chem. 23 (1984) 2936.
15. M. J. Kwiecien, L. Takacs and W. M. Reiff, Inorg. Chem. Paper No. 170, 193rd ACS Meeting, Denver, CO, April 1987.
16. W. Massa, Z. Kristallogr. 153 (1980) 201, and private conversation.
17. C. P. Landee, R. E. Greeney, W. M. Reiff, J. H. Zhang, J. Chalupa and M. A. Navotny, J. Appl. Phys. 57, 3343 (1985) and Phys. Rev. B xxxx (1989).
18. R. C. Thiel, H. DeGraff and L. J. De Jongh, Phys. Rev. Lett. 47, 1415 (1981).
19. C. E. Johnson, Proc. Phys. Soc. 88, 943 (1966).
20. S. Chandra and G. R. Hoy, Phys. Lett. 22, 254 (1966).
21. J. H. Zhang, W. M. Reiff, J. Miller and J. Calabrese, Inorg. Chem. Paper No. 169, 193rd ACS Meeting, Denver, CO, April 1987.